PHYSICAL REVIEW B VOLUME 6, NUMBER 11 1 DECEMBER 1972

Fluctuation Contributions to the Heat Capacity of Amorphous Superconducting Films*

G. D. Zally†‡ and J. M. Mochel§
Department of Physics and Materials Research Laboratory, University of Illinois, Urbana, Illinois 61801
(Received 15 May 1972)

The heat capacities of superconducting amorphous films have been measured near the transition temperature. The films, of bismuth-antimony alloy, had an area of 0.5 cm^2 and thickness ranging from 150 to 1350 Å. An ac temperature calorimetric technique was employed. Fluctuation contributions to the heat capacity were observed. Resistivity measurements of the same films displayed the same fluctuation effects reported by other authors. The temperature dependence of the fluctuation heat capacity was consistent with a behavior of (reduced temperature)$^{-1}$ and had the same width as the resistive transition. No singular behavior near T_c was observed. The temperature dependence close to T_c predicted by Masker, Marcelja, and Parks was not seen. The rounding of the transition can be understood by a Hartree-like theory first proposed by Gunther and Gruenberg.

I. INTRODUCTION

Over the past several years, a great deal of interest has developed in the area of phase transitions and the behavior of both static and dynamic properties near the critical point.[1] In particular, much theoretical and experimental work has been devoted to the nature of the superconducting transition.[2] Historically, the superconducting transition has been found to be somewhat different from other second-order phase transitions because it was described so very well by a mean-field or Landau[3]-type of theory. For fluids and magnetic systems, the mean-field results are not valid at temperatures near the transition.

The breakdown of mean-field theory for liquids and magnetic materials has been attributed to the presence of thermodynamic fluctuations, which are ignored in mean-field theory. Thus the heat capacity of liquid helium at the superfluid transition has a λ-like singularity which is spread out over several tenths of a degree, in contrast to the classically predicted discontinuity observed for bulk superconductors. Ginzburg[4] investigated the question and showed the large difference in scale between superconducting and other transitions was one of scale rather than of fundamental nature. He estimated that for a pure superconductor, the mean-field theory was valid to within 10^{-15} K of the transition and that fluctuation-produced deviations were therefore unobservable.

A more complete analysis of the situation for a superconductor shows that fluctuation effects are more pronounced in dirty superconductors than in pure. In addition, reduction of one or more of the dimensions below the fundamental length of the problem, the temperature-dependent coherence length $\xi(T)$, greatly enhances fluctuations. For thin films of amorphous superconductors, the critical behavior is spread over millidegrees or more.

In Sec. II mean-field results for superconductors are reviewed, and their range of validity for different geometries and materials are estimated. Theoretical work on fluctuations in superconductors is examined, and the results predicted by various theories for the electrical resistivity and the heat capacity are given. A good deal of experimental work has been done on the resistive transition, and the agreement with theory is good.

Attempts to measure deviations from the classical specific heat have been carried out only in pure bulk superconductors. The results are negative, as predicted. The present work is an investigation of the heat capacity of very dirty thin films. Fluctuation effects are predicted and observed.

In Sec. III the choice of materials is discussed and the experimental procedures are described. The experimental results are given in Sec. IV, along with a description of the data analysis. Section V contains discussion and conclusions.

II. THEORY

A. Breakdown of Mean-Field Theory

The phenomenological Ginzburg–Landau (G-L) theory,[5] which is equivalent to the microscopic BCS theory[6] close to T_c,[7] predicts an abrupt drop to zero in the electrical resistivity at the transition and a discontinuity in the specific heat given by[8]

$$\Delta C = 9.4 N(0) k_B^2 T_c , \tag{1}$$

where $N(0)$ is the normal electron density of states at the Fermi surface and k_B is Boltzmann's constant.

The G-L theory can be used to estimate the importance of thermodynamic fluctuations and thus to

define the temperature region in which fluctuation effects dominate and departure from mean-field results can be expected. Ferrell[9] set the breakdown criterion by requiring that the temperature-dependent coherence length $\xi(T)$ be less than a characteristic length of the system. This condition defines a value ϵ_0 of the reduced temperature $\epsilon = |T - T_c|/T_c$ within which mean-field theory no longer applies. For bulk material, films, and filaments the results are

$$\epsilon_{03} = [2\xi^3(0)\,\Delta C/k_B]^{-2} \quad \text{(bulk)}, \tag{2}$$

$$\epsilon_{02} = [2\xi^2(0)d\,\Delta C/k_B]^{-1} \quad \text{(film of thickness } d\text{)}, \tag{3}$$

$$\epsilon_{01} = [2\xi(0)S\Delta C/k_B]^{-2/3} \quad \text{(filament of area } S\text{)}. \tag{4}$$

For pure materials, these estimates yield values of $\sim 10^{-12}$ for bulk superconductors, $\sim 10^{-6}$ for a 1000-Å film, and $\sim 2\times 10^{-5}$ for a 10^{-8}-cm^2 filament. These regions are so small that experimental observation of fluctuations would be impossible. The situation is greatly improved for dirty materials, where the coherence length is reduced to $\xi(0) = 0.85(\xi_0 l)^{1/2}$, with l the electronic mean free path. For a short-mean-free-path material such as amorphous bismuth,[10] the estimates are $\sim 10^{-4}$ for bulk, 1.5×10^{-3} for a 1000-Å film, and $\sim 10^{-4}$ for a 10^{-8}-cm^2 filament.

B. Resistive Transition

Close to the point where mean-field theory begins to break down ($\epsilon \sim \epsilon_0$), the fluctuations are relatively small and interactions between them can be ignored. The fluctuations can then be treated as a first-order perturbation to mean-field theory.

Above T_c the fluctuations are expected to form regions where the order parameter is nonzero and the conductivity should rise. Aslamazov and Larkin[11,12] (A-L) and others[9,13–15] have calculated the excess conductivity in the dirty limit to be

$$\frac{\sigma'}{\sigma_n} = 1.1\left(\frac{2}{lk_F}\right)^{3/2}\left(\frac{k_B T_c}{E_F}\right)^{1/2}\epsilon^{-1/2} \quad \text{(bulk)}, \tag{5}$$

$$\frac{\sigma'}{\sigma_n} = \frac{e^2}{16d\hbar\sigma_n}\,\epsilon^{-1} = \frac{1.85\epsilon^{-1}}{k_F^2 ld} \quad \text{(film)}, \tag{6}$$

$$\frac{\sigma'}{\sigma_n} = 5.4\left(\frac{2}{lk_F}\right)^{1/2}\left(\frac{E_F}{k_B T_c}\right)^{1/2}\epsilon^{-3/2} \quad \text{(filament)}, \tag{7}$$

where σ_n is the normal-state conductivity and E_F and k_F are the Fermi energy and wave number, respectively.

The A-L result of (6) fits the data of Glover[16] for Bi films and of Strongin *et al.*[17] for granular Al films. The ϵ^{-1} behavior is exhibited for $\sigma'/\sigma_n < 0.5$, that is, outside of the critical region. The width of the transition,

$$\epsilon_{A\text{-}L} = e^2/16d\hbar\sigma_n = R_\square^n\ 1.52\times 10^{-5},$$

scales as it should with the samples normal resistance per square, $R_\square^n = 1/\sigma_n d$, and the numerical match is good.

An additional contribution to the fluctuation conductivity of a type first proposed by Maki[18] with a momentum cutoff established through either an external or internal pair-breaking interaction[19] was first demonstrated by Crow *et al.*[20] For our system (amorphous $Bi_{0.4}Sb_{0.6}$) we are well into the dirty limit ($l \sim 1$ Å), and our analysis of resistivity and heat capacity are done only close to the transition. In these regimes this additional contribution will broaden the resistive transitions by less than a factor of 2. For an equilibrium parameter, such as heat capacity, no such broadening should occur.

Amorphous $Bi_{0.4}Sb_{0.6}$ is a strong-coupled superconductor and the paraconductivity could also be modified[21] from the A-L result to

$$\frac{\sigma'}{\sigma_n} = \frac{e}{16\hbar d\sigma_n}\,\frac{t_{\rm rel}}{t_{\rm rel\ BCS}}\,\epsilon^{-1}, \tag{8}$$

where $t_{\rm rel}$ is the characteristic relaxation time of the order parameter and $t_{\rm rel\ BCS}$ is that time for a weak-coupling superconductor. This ratio is $\frac{1}{2}$ for Pb, and yet experimental results of Crow *et al.* are very close to the uncorrected A-L result near T_c.

C. Heat-Capacity Transition

The first theoretical treatment of the heat capacity of a superconductor that went beyond the simple G-L approach was done by Thouless.[22] He found anomalous contributions to the specific heat of a pure bulk superconductor,

$$C_+ = 8.8\Delta C(k_B T_c/E_F)^2\epsilon^{-1/2} \quad (T > T_c), \tag{9}$$

$$C_- = 11.5\Delta C(k_B T_c/E_F)^2\epsilon^{-1/2} \quad (T < T_c). \tag{10}$$

The temperature region over which these contributions are the same order as ΔC is less than 10^{-12} K wide and hence unobservable for pure bulk samples.

In their classic paper which treated the resistive transition, Aslamazov and Larkin[12] also calculated the fluctuation effects on the specific heat. They considered only the case of a bulk sample above T_c. For a pure material, they found the same result as Thouless, while for a dirty superconductor, they obtained

$$C_+ = 1.25\Delta C\left(\frac{k_B T_c}{E_F}\right)^{1/2}(k_F l)^{-3/2}\epsilon^{-1/2} \quad (l \ll \xi_0). \tag{11}$$

This expression for $C_+/\Delta C$ is within a numerical factor of their expression for σ'/σ_n. Thus fluctuation corrections in specific heat become important at the same temperatures at which the conductivity corrections become significant.

Although A-L did not extend their calculations to

the two-dimensional case, Ferrell[9] treated both three and two dimensions. His results for the bulk are the same as (11). In two dimensions Ferrell found

$$\frac{C_+}{\Delta C} = \frac{\pi}{9.4}\frac{E_F}{k_B T_c}\frac{1}{k_F^3 d\xi^2(0)}\epsilon^{-1} . \tag{12}$$

In the pure and dirty limits, this becomes

$$\frac{C_+}{\Delta C} = 4.7\frac{k_B T_c}{E_F}\frac{1}{k_F d}\epsilon^{-1} \qquad (l \gg \xi_0) , \tag{13}$$

$$\frac{C_+}{\Delta C} = \frac{1.28}{k_F^2 ld}\epsilon^{-1} \qquad (l \ll \xi_0) . \tag{14}$$

These are the same as the A-L relations for σ'/σ_n for films with reduced numerical coefficients.

Masker, Marcelja, and Parks[23] extended the first-order results by including another term in the G-L free energy and employing a Hartree type of approximation. The fourth-order term involves interactions between fluctuations and the calculation should hold closer to T_c. They present in their paper a preliminary calculation of the specific heat of a two-dimensional superconductor. Their results are presented graphically and are reproduced here in Fig. 1. The dotted lines are the mean-field result. Their curve represents a 500-Å-thick aluminum film with mean free path of 500 Å. The increments in the plot were $\epsilon \times 10^5$. Here the scale has been adjusted to $\epsilon \times 10^3$, which would be appropriate to a 500-Å-thick amorphous Bi film with 5-Å mean free path. The large rise in specific heat right at the transition, being several times ΔC in height and several millidegrees in breadth, should be experimentally observable. The high-temperature tail will follow the ϵ^{-1} behavior predicted by Ferrell.

Gunther and Gruenberg[24] also used a Hartree-type approximation of the fluctuation heat capacity near T_c. No divergence at T_c was obtained. Their result for two dimensions was

$$C_+[\xi(t)]/\Delta C = [1 + \xi_{G\text{-}L}^2/\xi^2\epsilon_0]^{-1} , \tag{15}$$

where

$$\frac{\xi_{G\text{-}L}^2}{\xi^2} = \epsilon + \epsilon_0 \ln\left(1 + \frac{q_c^2\xi_{G\text{-}L}^2}{\xi_{G\text{-}L}^2/\xi^2}\right) , \tag{16}$$

with $q_c \simeq 1/l$ and $\xi_0 = 0.31/k_F^2 ld$. $\xi_{G\text{-}L}$ is the G-L coherence length. For $T \gg T_c$ this result, up to a constant, is the same as (14). This approach has been put on a much stronger foundation by Patton.[25] In Sec. IV, Eq. (15) will be compared with our measurements.

Cochran[26] has conducted a very careful and complete set of experiments on pure bulk superconductors to search for anomalous contributions to the heat capacity of the type predicted by Thouless.[22] He has measured several samples of

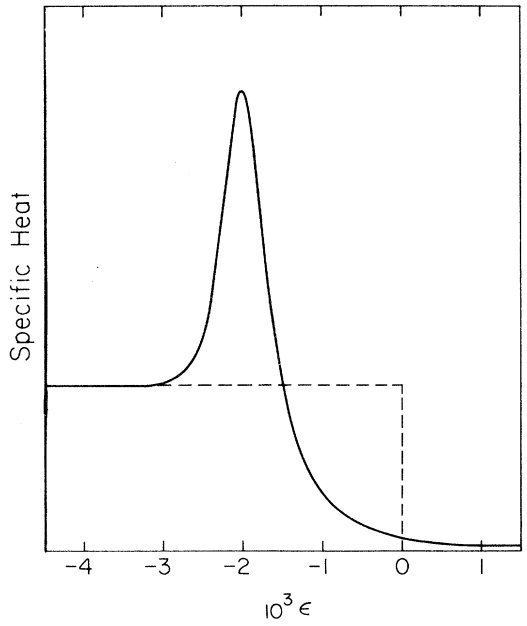

FIG. 1. Specific-heat anomaly predicted by Masker, Marcelja, and Parks for a 500-Å film with electronic mean free path of 5 Å. The plot corresponds to the total specific heat less that in the normal state. Dashed line: mean-field theory; $\epsilon = (T - T_c)/T_c$.

tantalum and tin and fit the data to the form

$$C(T) = C_0(T) + \alpha\epsilon^{-1} , \tag{17}$$

where $C_0(T)$ contains the mean-field discontinuity and the second term gives the contribution of fluctuations. He found that $\alpha = 0$ gave the best fit for all samples. That the experiments showed no anomalous contribution is understandable in light of the estimates of Thouless and others that the range of fluctuation effects would be 1×10^{-12} K for pure tin.

III. EXPERIMENTAL DETAILS

A. Materials

The amorphous superconductors first investigated by Buckel and Hilsch[27,28] comprise a group of very short mean-free-path materials for which fluctuation effects are expected to be important. In particular, when bismuth is deposited onto a cryogenic substrate it superconducts with a transition temperature of 6.1 K and has a mean free path[10] of 4.7 Å. Addition of antimony[29] to the bismuth depresses the transition temperature, reduces the mean free path, and increases the stability of the amorphous state against crystallization, which begins at ~15 K for the pure material. Transition temperatures vary continuously from 6.1 to 0 K at an antimony concentration of 70 at.%.

The alloys used, with a typical composition of

Bi + 60 at.% Sb, were made from 99.999% pure metal, the Bi from Johnson-Matthey and the Sb from ASARCO. The alloys were prepared at room temperature by melting the constituents in a quartz crucible *in vacuo*.

B. Substrate

The substrate for the evaporations consisted of a $\frac{1}{2}$-in. disk of thin (2–3 μm) Pyrex glass mounted on a copper heat sink which in turn was suspended inside the helium-bath heat shield of a demountable-tail cryostat. The glass separated the outer vacuum region from an inner region into which liquid helium could be bled via a needle valve. During evaporation, liquid helium at very low pressure was introduced behind the glass to prevent the substrate from warming up and causing the film to crystallize. Small grains of alloy were dropped into an evaporation boat and the Bi-Sb alloy film was deposited into the glass through shutters in the heat shields. The boat was 11 cm from the substrate. A mask restricted the metal deposition to a $\frac{5}{16}$-in. dot in the center of the substrate. Film thickness was controlled by evaporating a measured amount of alloy and was checked after the apparatus was disassembled by optical interferometry. After the evaporation, the region behind the glass was evacuated in order to thermally isolate the film for heat-capacity measurements.

A cross-section view of the substrate is shown in Fig. 2 and a bottom view in Fig. 3. Before the substrate is placed in the cryostat, a 100-Å constantan heater is evaporated onto the Pyrex with 400-Å gold leads extending to the perimeter. A 5000-Å layer of silicon monoxide is evaporated on top of the heater to insulate it from the Bi-Sb film. Four gold contacts for resistivity measurements extend to the edges of the region where the alloy film is to be placed. On the opposite side of the glass a 3000-Å dot of indium is evaporated in order to improve thermal diffusion over the region to be occupied by the alloy. A sample thermometer made from a small (1-mg) chip of Sb-doped Ge is sealed to the indium with Epoxy.

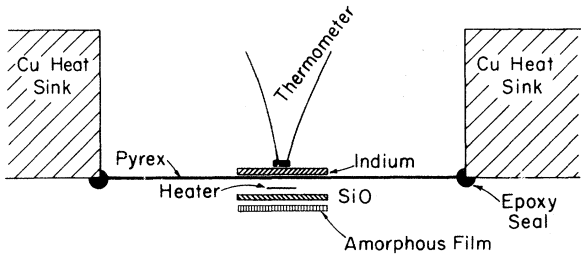

FIG. 2. Side view of sample holder and substrate.

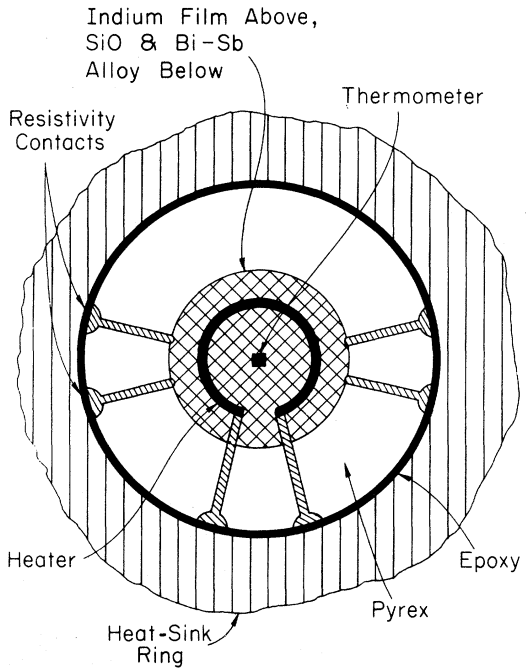

FIG. 3. Top view of sample holder and substrate showing heater and thermometer configuration, evaporated resistivity contacts, Pyrex window, and alloy dot.

At a transition temperature of 2.2 K for a typical sample, the heat capacity of the substrate assembly was about 1 erg/K. The size of the heat-capacity discontinuity, which sets the scale for fluctuation effects, was of the order of 0.01 erg/K for a 1000-Å Bi-Sb film. The small size of the heat capacities involved and the high accuracy required of the measurements precluded the use of adiabatic or continuous-heating calorimetry techniques.

C. ac Temperature Calorimetry

The basic features of the ac calorimetry technique[30,31] can be demonstrated by an examination of the simplified model of the experiment shown in Fig. 4. Consider a sample with heat capacity C_s and instantaneous temperature $T_s(t)$. A sinusoidally varying current $I_0\cos(\frac{1}{2}\omega t)$ drives a heater of resistance R_0 on the sample. The power delivered to the sample is $I_0^2 R_0 \cos^2(\frac{1}{2}\omega t)$. The sample is connected to a thermal bath held at temperature T_0 via a thermal link of total conductivity K_b. The steady-state solution for the sample temperature is given by

$$T_s(t) = T_0 + \Delta T + T_{ac}\cos(\omega t - \alpha)\ , \tag{18}$$

with the dc temperature rise ΔT, the amplitude of the ac temperature oscillations T_{ac}, and the phase shift of the oscillations α. The results are

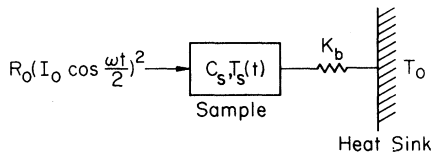

FIG. 4. Diagram of sample connected to a heat sink through thermal conductance K_b. Heat input to the sample is $\frac{1}{2}I_0^2R_0 \cos^2(\frac{1}{2}\omega t)$.

$$\Delta T = \dot{Q}_0/K_b \ , \tag{19}$$

where $\dot{Q}_0 = \frac{1}{2}I_0^2R_0$ is the average power input,

$$\alpha = \arcsin(1 + 1/\omega^2\tau^2)^{-1/2} \ , \tag{20}$$

and

$$T_{ac} = (\dot{Q}_0/\omega C_s)(1 + 1/\omega^2\tau^2)^{-1/2} \ , \tag{21}$$

where $\tau = C_s/K_b$ is the sample-to-bath relaxation time. If the frequency ω is chosen so that $\omega\tau \gg 1$, then $T_{ac} = \dot{Q}_0/\omega C_s$ and measuring the amplitude of the temperature oscillations gives a direct measurement of the reciprocal of the heat capacity.

The sample analysis above ignores a number of things that occur in a real experiment. The heater and thermometer each have their own heat capacities and are connected to the sample via finite thermal conductances. The temperature actually measured is that of the thermometer. In addition, the sample does not have infinite thermal conductivity. Sullivan and Seidel[31] have analyzed this situation and their result reduces to the form of (18) but with an additional term,

$$T_{ac} = \frac{\dot{Q}_0}{\omega C_{tot}} \left(1 + \frac{1}{\omega^2\tau_s^2} + \omega^2\tau_{int}^2\right)^{-1/2} \ . \tag{22}$$

Here C_{tot} is the heat capacity of the sample, heater, thermometer, and a portion of the thermal link. The sample-to-bath relaxation time is τ_s, and τ_{int} is an internal relaxation time that lumps time constants for sample-to-heater and sample-to-thermometer relaxation as well as sample-thermal-diffusion effects. The experiment was designed so that $\tau_s \gg \tau_{int}$ and a frequency could be found for which $\omega\tau \gg 1$ and $\omega\tau_{int} \ll 1$, with the result that the heat capacity is obtainable from T_{ac} measurements.

D. Instrumentation

The resistance of the sample thermometer was measured on an ac inductance bridge with a lock-in null detector. The heat-sink temperature was measured and controlled with a similar bridge to a reduced temperature of 5×10^{-6}. Both resistivity and heat-capacity measurements were made for each film.

The resistivity measurements were made with a four-probe method. The measurements were made point by point as a function of temperature. Measuring current densities were of the order of 0.5 A/cm^2. Measurements with current densities 10 times smaller gave the same results.

The heat-capacity measurements were made by applying a sinusoidal signal to the sample heater and monitoring the amplitude of the resultant temperature oscillations. Since the sample thermometer was in an ac bridge balanced about the steady-state resistance value, the error signal of the bridge oscillated at the frequency of the temperature oscillations. In order to measure the oscillation amplitude directly, a double-sideband signal was generated with sharp peaks at frequencies $f_t + f_0$ and $f_t - f_0$, where f_t was the bridge excitation frequency and f_0 the temperature oscillation fre-

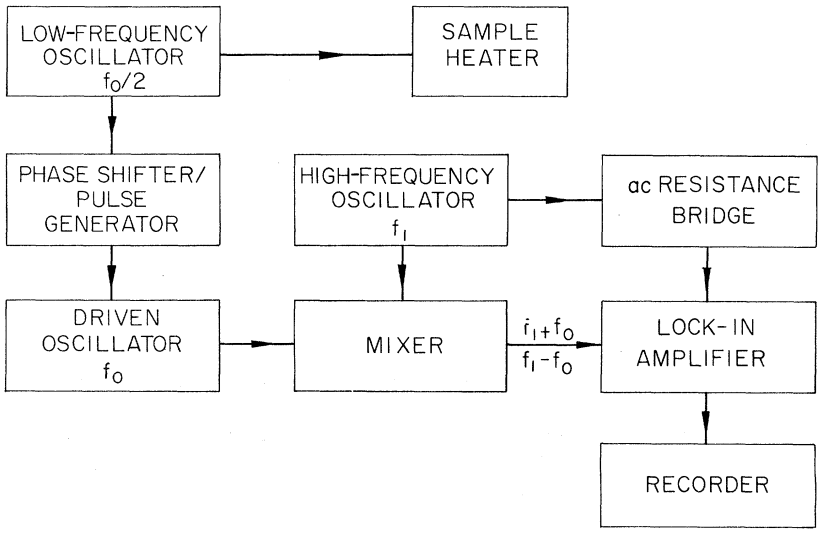

FIG. 5. Schematic diagram of the components comprising the electronic instrumentation for heat-capacity measurements. When a dc signal is fed into the mixer ($f_0 = 0$), the lock-in amplifier measures bridge balance.

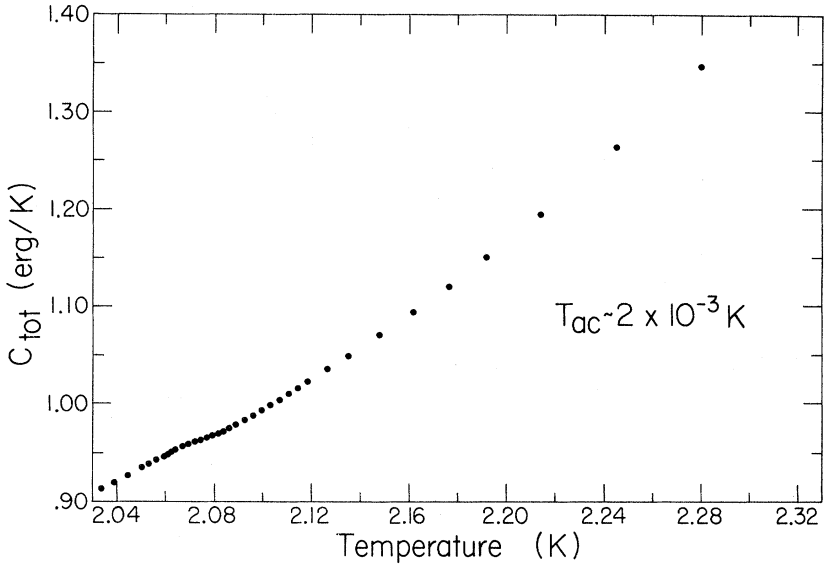

FIG. 6. Data for sample No. 18 after having been converted to heat capacity of the total sample vs temperature.

quency. This signal was fed into the reference input of the lock-in amplifier. The lock-in's integrated output was then proportional to the rms amplitude of the temperature oscillations. A schematic of the apparatus is shown in Fig. 5.

The level of the heating current and the bridge-measuring current were kept low enough so that temperature gradients across the sample were small compared to the amplitude of the temperature oscillations. Signal-to-noise characteristics were high enough so that instrument drift was the limiting factor in the measurements. Consistent measurements accurate to 1 part in 1500 were possible with the apparatus. A complete set of data was taken within a few hours to reduce the possibility that long-term changes in the sample heat capacity caused by variation in the amount of

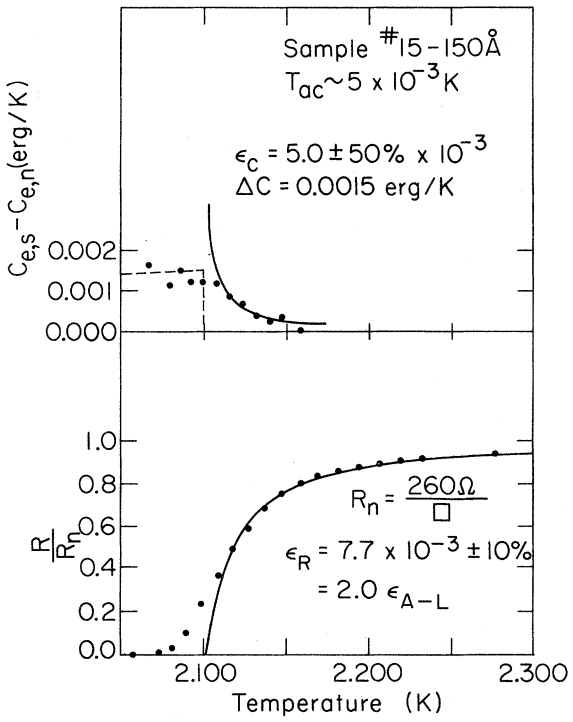

FIG. 7. Resistive and heat-capacity transitions for 150-Å Bi+60 at.% Sb film. Upper curve: fit to $C' = \Delta C(\epsilon_c/\epsilon)$. Lower curve: fit to $R = R_n(1+\epsilon_R/\epsilon)^{-1}$. Dashed curve: mean-field result.

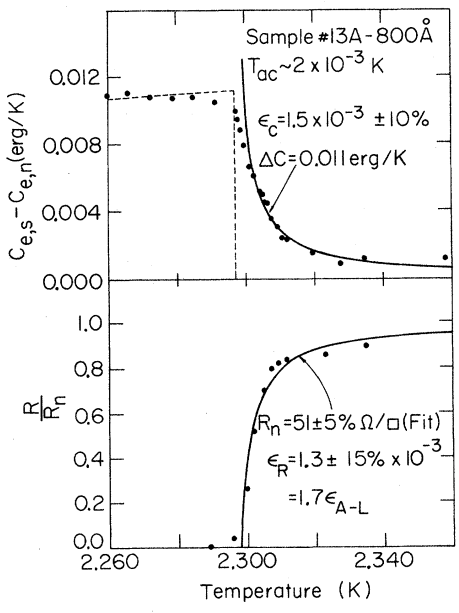

FIG. 8. Resistive and heat-capacity transitions for 800-Å Bi+60 at.% Sb film. Upper curve: fit to $C' = \Delta C(\epsilon_c/\epsilon)$. Lower curve: fit to $R = R_n(1+\epsilon_R/\epsilon)^{-1}$. Dashed curve: mean-field result.

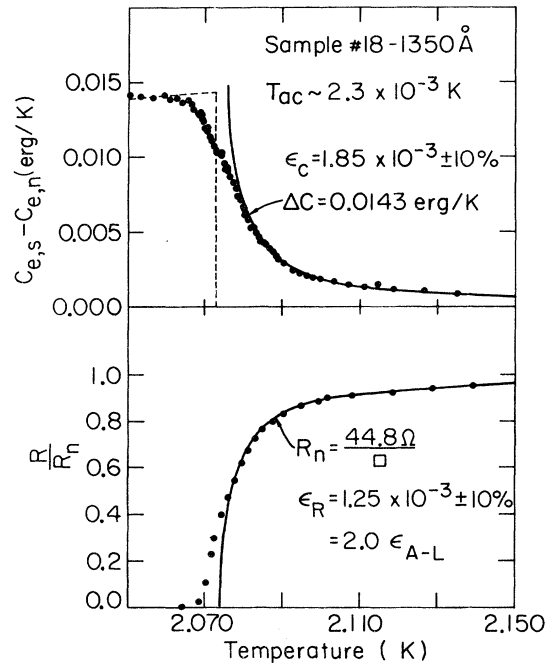

FIG. 9. Resistive and heat-capacity transitions for 1350-Å Bi+63 at.% Sb film. Upper curve: fit to $C' = \Delta C(\epsilon_c/\epsilon)$. Lower curve: fit to $R = R_n(1+\epsilon_R/\epsilon)^{-1}$. Dashed curve: mean-field result.

adsorbed helium gas might distort the results. The submonolayer of helium could never be completely eliminated.

IV. ANALYSIS AND RESULTS

The raw data were converted into heat-capacity values using measured ac bridge sensitivity and thermometer calibration. Figure 6 shows the heat capacity of sample No. 18 as a function of temperature.

In order to examine the fluctuation effects it was necessary to subtract the background heat capacity of the substrate and the lattice and normal electronic heat capacity of the Bi-Sb alloy film. This background heat capacity was fitted to the form

$$C_{\text{background}} = AT + BT^2 + CT^3 + DT^4 \ . \tag{23}$$

The coefficients of (23) were adjusted to fit the data well above T_c, where fluctuation effects could be ignored, and to a BCS form for $C_{e,s} - C_{e,n}$, the difference between the alloy electronic heat capacity in the superconducting and normal states, well below T_c.

Results for three alloy films of thicknesses 150, 800, and 1350 Å, are presented in Figs. 7–9. Both resistive and heat-capacity data are shown. The solid curve on each resistive transition is a fit to $R/R_n = (1+\epsilon_R/\epsilon)^{-1}$. The values of $R_\square^n$ and ϵ_R are indicated, and ϵ_R is compared with the A-L result, $\epsilon_{A-L} = 0.152 \times 10^{-4}\, R_\square^n$. All of the transitions are wider than the predicted width. If the broadening due to the Maki term is removed and dimensionality considered, then the width of the resistive transitions can be understood. The heat-capacity transitions are shown by a plot of the difference between the superconducting and normal-state electronic heat capacities $C_{e,s} - C_{e,n}$ against temperature. The dotted curve shows the behavior predicted by mean-field theory for each film, while the solid curve is a fit to $C' = \Delta C(\epsilon_c/\epsilon)$. The values of ΔC and ϵ_c are indicated. The values of T_c used to fit the heat capacity and resistive data were within 2 mK for each sample. The widths of

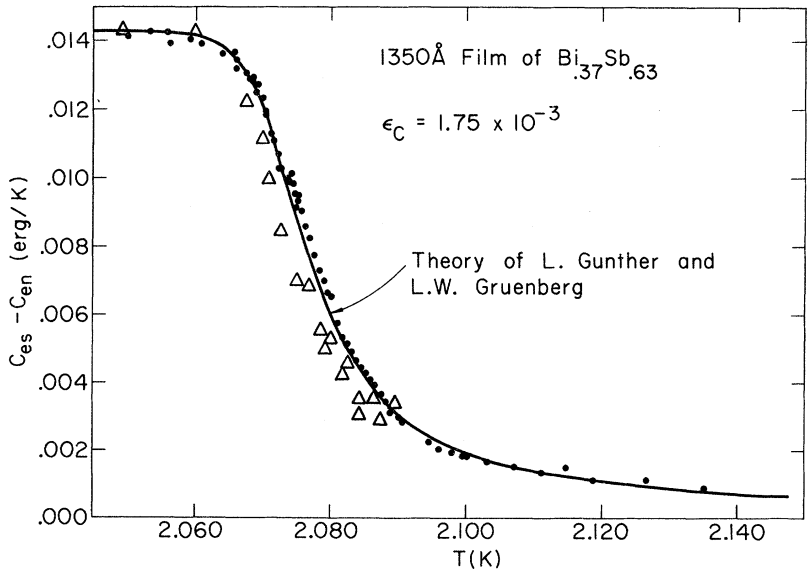

FIG. 10. Two-parameter fit between the Hartree-like theory of Gunther and Gruenberg and the fluctuation heat capacity in a 1350-Å film of $Bi_{0.37}Sb_{0.63}$. The resulting standard deviation is less than 3% but the width $\epsilon_c = 1.75 \times 10^{-3}$ is three times larger than expected on the basis of resistivity measurements. The open triangles are measurements taken with ΔT_{ac} five times smaller (0.5 mK) than the ΔT_{ac} for the solid points. There is only a slight sharpening of the transition due to the improved temperature resolution.

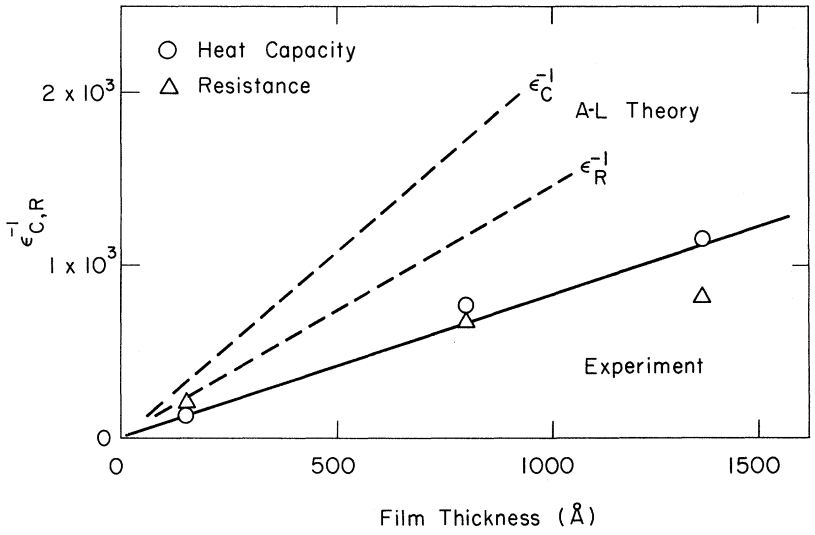

FIG. 11. Plot of ϵ_c^{-1} and ϵ_R^{-1} for the resistive and heat-capacity transitions vs film thickness. ϵ_c^{-1} is normalized by normal-state resistivity. On the basis of $R_\square^n$ and Eqs. (6) and (14) the dotted lines are plotted. The difference in the dotted line ϵ_R^{-1} and the experiment can be understood through the Maki–Thomson and thick-film corrections.

the resistive and heat-capacity transitions are of the same size for each film, with a few exceptions which are explainable in terms of scatter in the data. The uncertainty of the fits were ± 10% for ϵ_R (resistance) and ± 10% for ϵ_c (heat capacity), except as noted on the figures. The resistive data for sample No. 13A were noisy due to poor contact between the gold leads and the alloys. The heat-capacity data for the 150-Å film, sample No. 15, also have larger scatter due to the small size of the resultant signal and consequent lower signal to noise.

Heat-capacity measurements were made with the size of temperature oscillations indicated and were repeated with oscillations five times smaller. The results were essentially the same, as indicated in Fig. 10. It is only important that $T_{ac} \ll T - T_c$. The data show no indication of a singularity near T_c, nor do they exhibit the behavior predicted by Masker, Marcelja, and Parks[23] as shown in Fig. 1.

The ϵ^{-1} dependence of the fluctuation-produced conductivity was verified. The excess heat-capacity data were consistent with the ϵ^{-1} dependence predicted, but the high-temperature data required to verify this behavior were not accurate enough. Small changes in the subtraction of the background made significant changes in the shape of the high-temperature tail.

A detailed comparison between (15) and the fluctuation heat capacity of sample No. 18 is shown in Fig. 10. This is a two-parameter fit and results in a standard deviation of less than 3%. From this fit, $\epsilon_c = 1.75 \times 10^{-3}$ in contrast to predicted value of 0.11×10^{-3} or from calculation of Ferrell [Eq. (14)] of 0.47×10^{-3}. Since the film thickness for the 1350-Å film is greater than the coherence length the characteristic width of the transition will be decreased away from T_c. Most useful is a direct comparison of the widths of the heat-capacity transitions to the resistance $R_\square^n$. On this basis ϵ_c averages three times larger than expected from the ratio of (14) to (6) if the Maki–Thompson contribution (inferred from $R_\square^n$) is removed from the resistive transitions.

V. CONCLUSIONS

The heat capacity of thin superconducting films has been measured near the transition temperature. Deviations from the discontinuity predicted by mean-field theory have been observed, and these are attributed to the effects of thermodynamic fluctuations in the order parameter. Sufficiently far away from the critical temperature, the fluctuation heat capacity is consistent with the theoretically predicted ϵ^{-1} temperature dependence, but the data were not accurate enough over a wide enough range to verify the value of the exponent. The width of the transition was of the same order as the width of the resistive transition.

The A-L result as interpreted by Ferrell[9] predicts that the width of the fluctuation-heat-capacity transition should be 0.69 that of the resistivity transition. However, the widths of the heat-capacity transitions are equal to the resistive-transition widths for our system. If the Maki contribution is removed from the resistive transitions then the widths of the heat-capacity transitions are twice the widths of the resistive transitions.

We have demonstrated that it is possible to observe fluctuation heat capacity in a superconductor, and that no peaking of the heat capacity at T_c is produced in two dimensions.

*Research supported in part by the Advanced Research Projects Agency under Contract No. HC 15-67-C-0221.

†United States Steel Industrial Fellow.

‡Present address: Bell Telephone Laboratories, Holmdel, N. J. 07733.

§Alfred P. Sloan Fellow.

[1]L. P. Kadanoff, W. Götze, D. Hamblen, R. Hecht, E. A. S. Lewis, V. V. Palciauskas, M. Rayl, and J. Swift, Rev. Mod. Phys. 39, 395 (1967).

[2]*Proceedings of the Conference on Fluctuations in Superconductors, Asilomar, California*, edited by W. S. Goree and F. Chilton (Stanford Research Institute, Stanford, Calif., 1968).

[3]L. D. Landau and I. M. Lifshitz, *Statistical Physics* (Pergamon, London, 1958), Chap. XIV.

[4]V. L. Ginzburg, Fiz. Tverd. Tela 2, 2031 (1960) [Sov. Phys. Solid State 2, 1824 (1960)].

[5]V. L. Ginzburg and L. D. Landau, Zh. Eksperim. i Teor. Fiz. 20, 1064 (1950).

[6]J. Bardeen, L. N. Cooper, and J. R. Schrieffer, Phys. Rev. 108, 1175 (1957).

[7]L. P. Gor'kov, Zh. Eksperim. i Teor. Fiz. 36, 1918 (1959) [Sov. Phys. JETP 9, 1364 (1959)].

[8]A. A. Abrikosov, L. P. Gor'kov, and I. E. Dzyaloshinski, in *Methods of Quantum Field Theory in Statistical Physics*, translated and edited by R. Silverman (Prentice-Hall, Engelwood Cliffs, N. J., 1963), p. 306.

[9]R. A. Ferrell, J. Low Temp. Phys. 1, 241 (1969).

[10]J. S. Shier and D. M. Ginsberg, Phys. Rev. 147, 384 (1966).

[11]L. G. Aslamazov and A. I. Larkin, Phys. Letters 26A, 238 (1968).

[12]L. G. Aslamazov and A. I. Larkin, Fiz. Tverd. Tela 10, 1104 (1968) [Sov. Phys. Solid State 10, 875 (1968)].

[13]H. Schmidt, Z. Physik 216, 336 (1968).

[14]E. Abrahams and J. W. F. Woo, Phys. Letters 27A, 117 (1968).

[15]L. P. Kadanoff and G. Laramore, Phys. Rev. 175, 579 (1968).

[16]R. E. Glover, Phys. Letters 25A, 542 (1967).

[17]M. Strongin, O. F. Kammerer, J. Crow, R. S. Thompson, and H. L. Fine, Phys. Rev. Letters 20, 922 (1968).

[18]K. Maki, Progr. Theoret. Phys. (Kyoto) 39, 897 (1968); 40, 193 (1968).

[19]R. S. Thompson, Phys. Rev. B 1, 327 (1970).

[20]J. E. Crow, R. S. Thompson, M. A Klenin, and A. K. Bhatnagar, Phys. Rev. Letters 24, 371 (1970).

[21]P. Fulde and K. Maki, Physik Kondensierten Materie 8, 371 (1969).

[22]D. Thouless, Ann. Phys. (N. Y.) 10, 553 (1960).

[23]W. E. Masker, S. Marcelja, and R. D. Parks, Phys. Rev. 188, 745 (1969).

[24]L. Gunther and L. W. Gruenberg (unpublished).

[25]Bruce R. Patton, Phys. Rev. Letters 27, 1273 (1971); and unpublished.

[26]J. F. Cochran, Ann. Phys. (N. Y.) 19, 186 (1962).

[27]W. Buckel and R. Hilsch, Z. Physik 131, 420 (1952).

[28]W. Buckel and R. Hilsch, Z. Physik 138, 109 (1954).

[29]N. Barth, Z. Physik 142, 58 (1955).

[30]P. Handler, D. E. Mapother, and M. Rayl, Phys. Rev. Letters 19, 356 (1967).

[31]P. Sullivan and G. Seidel, Phys. Rev. 173, 679 (1968).